

Formation of TiC-core, graphitic-mantle grains from CO gas

Yuki Kimura^{1*}, Joseph A. Nuth III¹, and Frank T. Ferguson^{1,2}

¹Astrochemistry Laboratory, Code 691, Solar System Exploration Division, NASA
Goddard Space Flight Center, Greenbelt, MD 20771, USA

²Dept. of Chemistry, Catholic University of America, Washington, DC 20064, USA

*Corresponding author's e-mail address: ykimura@ssedmail.gsfc.nasa.gov

Abstract

We demonstrate a new formation route for TiC-core, graphitic-mantle spherules that does not require c-atom addition and the very long timescales associated with such growth (Bernatowicz et al. 1996). Carbonaceous materials can also be formed from C_2H_2 and its derivatives, as well as from CO gas. In this paper, we will demonstrate that large cage structure carbon particles can be produced from CO gas by the Boudouard reaction. Since the sublimation temperature for such fullerenes is low, the large cages can be deposited onto previously-nucleated TiC and produce TiC-core, graphitic-mantle spherules. New constraints for the formation conditions and the timescale for the formation of TiC-core, graphitic-mantle spherules are suggested by the results of this study. In particular, TiC-core, graphitic-mantle grains found in primitive meteorites that have never experienced hydration could be mantled by fullerenes or carbon nanotubes rather than by graphite. In situ observations of these grains in primitive anhydrous meteoritic matrix could confirm or refute this prediction and would demonstrate that the graphitic mantle on such grains is a metamorphic feature due to interaction of the pre-solar fullerenes with water within the meteorite matrix.

1. Introduction

The formation environment of TiC-core, graphitic-mantle spherules was calculated after their discovery in acid residues derived from the Murchison carbonaceous meteorite. (Bernatowicz et al. 1991). The graphitic spherules including metal carbide crystals such as TiC were identified as presolar grains from their isotopic content and assumed to form within the circumstellar envelopes of carbon-rich asymptotic giant branch (AGB) stars (Bernatowicz et al. 1991, 1996). The metal carbide crystals were composed of Ti and/or Zr-Mo carbide, were generally located at the center of individual spherules and are surrounded by well-graphitized carbon. Therefore, it had been assumed that TiC condensed prior to carbon. These composite spherules have been called core-mantle grains. The radii of the metal carbide core and of the graphitic mantle layer are 5-200 nm and 0.3-9 μm , respectively. Constraints on the formation conditions and environment, such as the C/O abundance ratio and total gas pressure, of the TiC-core, graphitic-mantle spherules can be derived from the size of the TiC core and graphitic mantle, and depend on the vapor density and the cooling rate of the grains.

Initially, using thermodynamic equilibrium calculations, the C/O abundance ratio and total gas pressure were constrained on the basis of the condensation sequence, i.e., TiC condenses prior to carbon (Lodders and Fegley 1995; Sharp and Wasserburg 1995). After that, non-equilibrium condensation theory (Yamamoto and Hasegawa 1977; Draine and Salpeter 1977; Kozasa and Hasegawa 1987) was applied to clarify the formation conditions of TiC cores and graphitic mantles from the constraints derived from the sizes of their spherules, in addition to the condensation sequence (Chigai et al. 1999). Even then, however, it was difficult to explain the thickness of the graphitic

mantle layer based on the typical physical conditions expected in the circumstellar envelopes of carbon stars, namely the calculated thickness of the graphite mantle is close to the lower limit of the observed size. They assume that this difficulty derives from their simple treatment of the condensation process for graphite mantles, which uses all C_2H_2 molecules available for the formation of the graphite, accreted without the energy barrier for heterogeneous nucleation, onto the precondensed TiC grains that had grown independently (Chigai et al. 2002). Bernatowicz et al. (1996) estimated that even if every carbon atom that hit the growing mantle were incorporated into the final grain, growth would require approximately one year under equilibrium conditions at 0.1 dynes/cm^2 for a grain density of $3 \times 10^{-4} \text{ cm}^{-3}$. Michael, et al. (2003) demonstrated that perfect sticking is unlikely to have occurred and that growth of the largest grains may have required nearly 10^5 years. Since the graphite mantle is condensed on the surfaces of precondensed TiC grains, the sizes of the TiC core and the graphitic mantles depend on the heterogeneous condensation temperature of graphite and on the concentration of C_2H_2 molecules available for heterogeneous condensation.

Recently, detailed calculations have been carried out that consider both heterogeneous nucleation on the pre-condensed TiC grain surfaces and homogeneous nucleation of graphite in the gas phase (Chigai et al. 2002). As a result, they showed that the constraints imposed by the gas outflow velocity, stellar mass loss rate, total gas pressure and C/O abundance ratio matched those at the nucleation and growth site of TiC-core, graphitic-mantle spherules admirably. In addition, it has been suggested that when TiC condenses prior to graphite, the homogeneous condensation of graphite grains does not occur. It has also been suggested that TiC-core, graphitic-mantle spherules

can be formed at an earlier stage of low mass loss rates in addition to the superwind stage (Chigai et al. 2002). If these grains actually do form on 10^5 year timescales (Michael et al 2003), then grain formation must definitely occur prior to the start of mass loss.

Most of the carbon in the outflow of carbon-rich AGB stars is in the form of CO and C_2H_2 (Latter 1991). Carbonaceous materials such as polycyclic aromatic hydrocarbons (PAHs) and fullerenes are believed to form from C_2H_2 and its derivatives because CO is a very stable molecule (Allamandola et al. 1987, 1989). Therefore, all of the theoretical calculations described above were carried out based on C_2H_2 gas abundances, i.e., no one has ever considered CO gas as a carbon source. If carbonaceous materials are formed not only from C_2H_2 molecules but also from CO gas, then most predicted formation constraints such as gas outflow velocity, stellar mass loss rate, total gas pressure temperature and C/O abundance ratio will require reconsideration. Here we demonstrate the production of carbonaceous materials from CO gas in the laboratory and present a possible new formation route for TiC-core, graphitic-mantle spherules around AGB stars.

2. Experimental Procedure

Carbon and/or titanium carbide smoke particles were prepared in our laboratory by a modified gas evaporation method using the Graphitic Smokes Apparatus. The apparatus used was a glass chamber 32 cm in diameter and 32 cm in height and connected to a vacuum exhaust through a valve at its bottom. The main pieces around

the evaporation source are made of carbon built on a stainless steel foundation, which does not become hotter than 100°C during the course of an experiment. Smoke grains were produced at a total pressure of 200 Torr, which was measured using a diaphragm gauge, in a gas mixture of He and CO. After first evacuating the apparatus using a mechanical pump, He or CO gas was introduced to a pressure of about 100 Torr. After that, the gas was evacuated once again, and He and CO gas were introduced carefully up to their objective partial pressures. Since the ambient He gas is heated and CO gas is decomposed during the resistive heating of the carbon rod, the total pressure varies and increases to about 220 Torr by the end of experiment. A carbon electrode (55 mm, 6.35 mm ϕ), with a thinned section (16 mm, 3 mm ϕ) at the middle, was prepared and vaporized via resistive heating. The temperature was kept relatively constant by controlling the current. Since the vapor pressure of carbon is just about 1 Torr at a temperature of roughly 2700-3000°C, and between 0.1 and 1 torr of condensable vapor is often required to form smokes, we estimate that the temperature of the carbon rod was at least 2700°C. The resistively heated carbon rod induced a severe thermal gradient into the ambient gas. Therefore, the vapor leaving the resistively heated rod subsequently cools and condenses rapidly to form smoke particles in the ambient gas. The carbon particles produced were collected onto a stainless-steel plate, which is kept below 100°C, 8 cm above the evaporation source during these very short runs.

In the case of TiC particle production, Ti wire (Alfa Aesar, A Johnson Matthey Company, 0.5 mm ϕ , 99.98%) was wound around the thinned section of the carbon electrode. By pre-heating the carbon electrode in He gas, the Ti wire was heated and melted around the thinned section of the carbon electrode. As a result, the evaporation of carbon was suppressed (Kimura & Kaito 2003). After the Ti wire was melted onto

the carbon electrode, the apparatus was evacuated and filled with the experimental gas mixture.

A thirty-second run produced about 100 mg of black smoke. Ten samples of carbon and titanium carbide smoke particles were produced with five different ratios of He and CO gases in the mixture at pressures of 200 and 0, 150 and 50, 100 and 100, 50 and 150, and 0 and 200 Torr, respectively: twelve duplicate experiments were attempted.

The collected smoke samples were mounted on holey amorphous carbon thin films supported by standard 200-mesh Cu TEM grids. TEM observations were carried out using a JEOL 2010 TEM operated at an accelerating voltage of 200 keV at the University of New Mexico and a TOPCON 002B TEM operated at an accelerating voltage of 200 keV and a JEOL 4000EX TEM operated an accelerating voltage of 400 keV at The John M. Cowley Center for High Resolution Microscopy at Arizona State University.

Mid-infrared spectra from 700 to 400 cm^{-1} of collected smoke samples, embedded in KBr pellets, were measured with a Fourier-transform infrared spectrometer (Mattson Polaris FT-IR spectrometer). The infrared system utilized a KBr beam splitter and deuterated triglyceride sulfate detector. The energy resolution used for this work was 2 cm^{-1} .

3. Results and discussion

Since all of the collected carbon particles have the same black color, typical of

carbon soot, it looks like the same structural material. However, as a result of TEM observations, we found that the faces of those carbon particles were drastically different. The results of our TEM observations are summarized in Table 1. Figure 1 shows typical TEM images of carbon smoke particles produced under He and/or CO gas: (a) He 200 Torr, (b) He 150 and CO 50 Torr and (c) CO 200 Torr, respectively. The carbon particles in Fig. 1(a) are 50-100 nm in diameter, dendritic in shape, have smooth surfaces and cluster in the gas phase. The character of these carbon particles is similar to those of the amorphous carbon particles commonly produced in inert gas (Kaito et al. 1993). Although the size and shape of the carbon particles produced in a gas mixture of He 150 Torr and CO 50 Torr are similar to the carbon particles produced under He 200 Torr, the surface is rougher, as indicated by arrows in Fig. 1(b). The roughness of the particle surface could be caused by secondary reaction with the CO gas. With an increasing ratio of CO gas to He gas, the surfaces of these particles again become smooth. In particular, the size and face of the carbon particles produced in 200 Torr of CO gas are quite similar to those of carbon particles produced in 200 Torr of He gas, as shown in Fig. 1(c). However the structure of the carbon component is drastically different.

Figure 2 shows a high-resolution TEM (HRTEM) image and a corresponding electron diffraction (ED) pattern of the surface of a carbon particle in Fig. 1(b). Many large cages, which appear to be short nanotubes or large fullerenes, are visible. Although a typical ED pattern of a graphitic structure shows two rings corresponding to the (002) and (101) crystallographic planes, the ED pattern of our large cages show two different halo rings corresponding to the (100) and (110) planes, as shown in Fig. 2(b). This result means that the multiple layer structure typical of graphite crystals was not

produced in these grains. The carbon particles are random sized fullerenes. The layer structure, which corresponds to the (002) planes of the graphite crystal, was also not seen during HRTEM observations, as shown in Fig. 2(a). In addition, the carbon particles produced in 200 Torr of CO gas were sublimated during vacuum heating that reached temperatures as high as 800°C. This behavior is similar to, albeit it occurs at higher temperature than, the sublimation of the fullerenes, C₆₀ and C₇₀, at 300 and 350°C, respectively (Cox et al. 1991).

In order to supplementary confirm the presence of fullerenes, mid-infrared spectra were measured. However, it was difficult to find the characteristic infrared feature of fullerenes from the spectrum (a), which was taken from the specimens shown in Fig. 1, because the size of the carbon cages in the samples we produced are widely distributed, as seen in Fig. 2(a). We found that the size distribution of fullerene is concentrated to the small fullerenes by the use of titanium as catalyst. Titanium wire, which was wound around the thinned section of the carbon electrode, was evaporated in CO gas at 200 Torr without pre-heating in He gas. As a result, Ti wire is evaporated as Ti atoms rather than as TiC. The cage structure was observed to be quite similar in both carbon particle samples with and without Ti on the TEM images, and only the size of the cages produced with Ti was smaller as indicated by arrows in Fig. 3 (f). Spectra (b)-(d) were measured from the smaller cage dominant samples, which were made using three different amounts of Ti catalyst. We varied the Ti to C ratio by changing the length of Ti wire and the thickness of carbon rod used in the experiments. The amount of evaporated Ti is less in alphabetical order, i.e., (b) < (c) < (d). These infrared spectra showed a significant 19 μm feature (526 cm^{-1}), which is the strongest peak of C₆₀ in the mid-infrared region (Kimura et al. 2005), and the intensity of the 19 μm feature

decreased as the fraction of Ti decreased. Accordingly, it can be concluded that the Ti atoms accelerate the production of C_{60} . Since the intensity of the 19 μm feature of spectra (c) and (d) is same, it may be saturated. Decreasing the partial pressure of CO gas weakened the 19 μm feature. Accordingly, we conclude that the large cages are single shell structures, i.e., fullerenes of many sizes, but most are larger than C_{70} .

Figure 4 shows the HRTEM images of the carbon particles corresponding to Fig. 1. In the case of particles produced in 150 Torr of He and 50 Torr of CO, the large cages are visible only on the surface, as shown in Fig 4(b), i.e., the large cages are deposited on an amorphous carbon particle. On the other hand, in the case of particles produced in 100 Torr of He and 100 Torr of CO, large cages were distributed towards the inside of the particles, i.e., amorphous-carbon-core, large-cage-mantle. In the case of particles produced in 200 Torr of CO, an amorphous carbon core was no longer visible. Therefore, it seems that the large-cage-carbon particles were predominantly produced from the decomposition of CO gas as opposed to the amorphous-carbon grains produced via evaporation of the carbon rod.

Solid carbon and CO_2 gas are produced from the catalytic disproportionation of CO gas by the Boudouard reaction. In the 1970's, the Boudouard reaction was used to produce graphite flakes, lamellar graphitic crystallites and filamentous graphite using Mg, Ni, Fe, Co and Mo as catalytic metals (Baird et al. 1974; Trimm 1977). After two decades, single-walled carbon nanotubes were produced by the Boudouard reaction using CO gas at 1200°C and Mo particles as catalysts (Dai et al. 1996). Subsequently, the Boudouard reaction has been widely used in the production of carbon nanotubes using Mo, Ni, Co, Ni-MgO and Fe as catalytic metals (e.g., Chen et al. 1997; Nikolaev

et al. 1999). Our large cages include nanotube-like cages with 5-7 nm lengths and ~2 nm widths. Since there is no report that fullerenes or nanotubes with this size are produced by the common evaporation of a carbon rod, we believe that our large cage carbon particles were produced by the Boudouard reaction, but in a catalytic metal free system. In other words, since catalytic metal was not present, the large cage carbon particles were not grown as carbon nanotubes. The high temperature (~3000K) of the evaporation source would provide sufficient energy to induced the Boudouard reaction. Although we do use Ti wire to make TiC-core, graphitic-mantle grains, the production of large fullerenes was also observed to occur in Ti-free gas mixtures of He and CO and their formation was confirmed using TEM observations (Figure 1).

When the carbon rod is evaporated in an inert gas, a rising smoke cloud from the evaporation source can be observed. The motion of the particles follows convective currents produced by the hot rod. Large carbon particles grow by coalescence as a result of collisions among the carbon atoms and/or small particles and subsequently form clusters. The coalescence efficiency among the particles depends on the surface Debye temperature of the particles (Kaito 1985). Since the large cages are present only on the particles' surface in the case of production in a gas mixture of He and CO, the large cages are deposited after production of the amorphous carbon particles. Although the evaporation temperature of carbon is quite high (~3000 K), the sublimation temperature of fullerene-like carbon particles is very low. For example, the sublimation temperatures of C₆₀ and C₇₀ are 300 and 350°C, respectively (Cox et al. 1991). Therefore, even if amorphous carbon particles formed by the evaporation of the rod and large cages are simultaneously produced around the carbon rod by the Boudouard reaction, the amorphous-core, large-cage-mantle structure would be

produced due to the large difference in coalescence temperature (i.e, the large cages will remain in the gas-phase until the gas cools down to a considerable degree).

TiC grains were produced in a CO gas atmosphere in order to make analogs of TiC-core, graphitic-mantle spherules found in meteorites. Figures 5(a) and (b) show the TEM images of TiC grains produced in He gas at 200 Torr and in CO gas at 200 Torr, respectively. The sizes of both samples of TiC grains are similarly distributed between 20-40 nm whereas the thickness of the mantle layer is drastically different. Although the production conditions for both samples of TiC grains were the same except for the composition of the gas atmosphere, the mean thickness of the carbon mantle layer of TiC produced in CO gas is approximately 20 nm versus 2 nm for particles formed in He gas. Although the number density of Ti atoms is 10^{-4} times smaller than that of carbon atoms, as estimated from the relative volumes of the particles, TiC grains were grown to 20-40 nm. During gas evaporation, since the growth of TiC is terminated by the deposition of lots carbon atoms onto the surface of growing TiC grains, TiC grains cannot be grown larger than 20 nm in a carbon rich environment (see Fig. 1 in Kimura and Kaito 2003). Therefore, we believe that the growth of TiC was not prevented due to later deposition of fullerenes at low temperature. Certainly, the thickness of the mantle layer in these experiments is too small compared with the mantles in meteoritic grains. However, this result does not contradict our hypothesis, as the meteoritic grains would have had considerably more time to grow, even in the expanding atmosphere of an AGB star, than was available during our experiments. Although the expected pressures in circumstellar environments is 2-5 orders of magnitude lower than in this experiment, there is much more chance to grow a carbon mantle layer by the deposition of fullerenes onto the TiC grains due to their low sublimation temperature, if

fullerenes are produced in earlier stages of grain formation, i.e., in outflow of a carbon star or in the superwind phase terminating the life of the AGB star. We expect that one might estimate the possibility of this new formation route based on our experimental results.

The mantle layer over TiC grains found in meteorites consists of graphitic carbon while the carbonaceous mantle produced in our experiments is composed of large cage structures. Although buckminsterfullerene, C_{60} , is thermally stable up to over 4000°C , as shown by the molecular dynamics study of Zhang et al. (1993), C_{60} is transformed to graphitic amorphous carbon at only 400°C in the presence of water (Suchanek et al. 2001). Indeed, since the Murchison meteorite is classified as a CM2, we know that these TiC-core, graphitic-mantle spherules were exposed to a hydrothermal environment that could have transformed the large cage structures into amorphous graphitic carbon. Of course nothing precludes the earlier transformation of such cage structures to amorphous carbon by exposure to water vapor: such exposure could have occurred in the expanding atmosphere of the AGB star, in the molecular cloud core from which the Solar Nebula collapsed, or in the nebula itself. Therefore, we propose a possible new formation route; namely, that TiC-core, graphitic-mantle spherules are produced by the deposition of large pre-nucleated carbon cages onto TiC grains in the atmosphere of an AGB star and the subsequent hydrothermal alteration of the fullerenes to a graphitic structure. Nanocrystalline-core, well-graphitized carbon mantle spherules were also found in the Murchison meteorite (Bernatowicz et al. 1996). The nanocrystalline cores are constructed by randomly oriented graphene sheets with little graphitic layering order. Our hypothesis would be applied to the formation of this composite carbon grain.

Since there are many types of carbonaceous materials, such as PAHs, graphite with various degrees of order, amorphous carbons, fullerenes and carbides and their composite structures have been found in meteorites and in stellar sources, there could be basic building blocks that eventually form carbonaceous grains. Although it has been assumed that CO gas is very stable, it might actually be a very important source for the formation of carbonaceous grains.

If this scenario is correct, then there is the possibility that the site where hydrothermal alteration occurs could be determined; though this is only possible if the alteration occurs within the meteorite parent body. If TiC-core, carbonaceous-mantle grains could be detected in situ in the matrix of truly anhydrous primitive meteorites such as ALH77307 (CO3.0), Acfer 094 (unique), Adelaide (unique), Kakangari (K), Semarkona (LL3.0) (see Nuth, et al., 2005), then the structure of the carbonaceous mantle could be analyzed to distinguish between a graphitic or cage structure. If fullerene-like cages were found in such anhydrous matrices then such a detection would not only confirm the meteorite parent body as the site of hydrothermal metamorphism, but would also be a very strong argument that such core-mantle grains formed via the scenario outlined above.

4. Conclusion

Thermodynamic equilibrium calculations (Lodders and Fegley 1995, Sharp and Wasserburg 1995), non-equilibrium condensation theory (Chigai et al. 1999),

homogeneous and heterogeneous nucleation (Chigai et al. 2002) have all been applied to explain the formation of TiC-core, graphitic-mantle spherules. Since carbonaceous materials including fullerenes can be formed from C_2H_2 and its derivatives (Allamandola et al. 1987, 1989; Becker and Bunch 1997), the formation of TiC-core, graphitic-mantle spherules has also been theoretically modelled based on the abundance of C_2H_2 gas. We suggest that the TiC-core, graphitic-mantle spherules could have been produced by the deposition of large pre-nucleated carbon cages, formed via the Boudouard reaction from CO, that were then deposited onto TiC grain cores. These composites subsequently experienced hydrothermal alteration. Since the Boudouard reaction is accelerated by small metallic particles, large fullerene-like cages would be produced quite easily around AGB stars. We expect that new constraints on particle formation in AGB stars via the Boudouard reaction could be derived from detailed theoretical calculations based on our study. In particular, we suggest that TiC-core, graphitic-mantle grains found in primitive meteorites that have never experienced hydration could be mantled by fullerenes or carbon nanotubes rather than graphite. In situ observations of these grains in primitive anhydrous meteoritic matrix could confirm this prediction and would demonstrate that the graphitic mantle on such grains is a metamorphic feature due to interaction of the pre-solar fullerenes with water within the meteorite matrix.

Acknowledgements

TEM analysis was performed in the Electron Microbeam Analyses Facility of the Department of Earth and Planetary Sciences at the University of New Mexico, where Adrian J. Brearley and Ying-Bing Jiang provided technical support. We also gratefully

acknowledge the use of facilities within the Center for Solid State Science at Arizona State University. This work was partially supported by grants from Japan Society for the Promotion of Science (JSPS) Postdoctoral Fellowships for Research Abroad from April 2004 to March 2006 and from NASA's Cosmochemistry Research and Analysis Program.

References

- Allamandola L. J., Sandford S. A., and Wopenka B. 1987. Interstellar polycyclic aromatic hydrocarbons and carbon in interplanetary dust particles and meteorites. *Science* 237:56-59.
- Allamandola L. J., Tielens A. G. G. M., and Barker J.R. 1989. Interstellar polycyclic aromatic hydrocarbons- The infrared emission bands, the excitation emission mechanism, and the astrophysical implications. *ApJS* 71:733-775.
- Baird T., Fryer J. R., and Grant, B. 1974. Carbon formation on iron and nickel foils by hydrocarbon pyrolysis-reaction at 700°C. *Carbon* 12:591-602.
- Becker L., and Bunch T. E. 1997. Fullerenes, fulleranes, and PAHs in the Allende meteorite. *Meteoritics & Planetary Science* 32:479-488.
- Bernatowicz T. J., Amari S., Zinner E., and Lewis R. S. 1991. Interstellar grains within interstellar grains. *ApJ* 373:L73-L76.
- Bernatowicz T. J., Cowsik R., Gibbons P. C., Lodders K., Fegley B., Jr., Amari S., and Lewis R. S. 1996. Constraints on stellar grain formation from presolar graphite in the Murchison meteorite. *ApJ* 472:760-782.
- Chen, P., Zhang, H. -B., Lin, G. -D., Hong, Q., and Tsai, K. R. 1997. Growth of carbon nanotubes by catalytic decomposition of CH₄ or CO on a Ni-MgO catalyst. *Carbon* 35:1495-1501.
- Chigai T., Yamamoto T., and Kozasa T. 1999. Formation conditions of presolar TiC core-graphite mantle spherules in the Murchison meteorite. *ApJ* 510:999-1010.
- Chigai T., Yamamoto T., and Kozasa T. 2002. Heterogeneous condensation of presolar titanium carbide core-graphite mantle spherules. *Meteoritics & Planetary Science*

37:1937-1951.

- Cox D. M., Behal S., Disko M., Gorun S. M., Greaney M., Hsu, C. S., Kollin E. B., Millar J., Robbins J., Robbins W., Sherwood R. D., and Tindall P. 1991. Characterization of C₆₀ and C₇₀ clusters. *J. Am. Chem. Soc.* 113:2940-2944.
- Dai H., Rinzler A. G., Nikolaev P., Thess A., Colbert T., and Smalley R. E. 1996. Single-wall nanotubes produced by metal-catalyzed disproportionation of carbon monoxide. *Chem. Phys. Lett.* 260:471-475.
- Draine B., and Salpeter E. E. 1977. Time-dependent nucleation theory. *J. Chem. Phys.* 67:2230-2235.
- Kaito C. 1985. Coalescence Growth Mechanism of Smoke Particles. *Jpn. J. Appl. Phys.* 24:261-264.
- Kaito C., Kimura S., Sakamoto T., Yoshimura Y., Kaigawa R., Sakaguchi T., Nakayama Y., and Saito Y. 1993. Fullerene crystal prepared by evaporating amorphous carbon rod in inert gas. *J. Crystal Growth* 134:157-161.
- Kimura Y., and Kaito C. 2003. Titanium carbide particles as pre-solar grains. *Mon. Not. R. Astron. Soc.* 343:385-389.
- Kimura Y., Nuth III J. A., and Ferguson F. T. 2005. Is the 21-mm feature observed in some post-AGB stars caused by the interaction between Ti atoms and fullerenes? *ApJL* 632:L159-L162.
- Kozasa T., and Hasegawa H. 1987. Grain formation through nucleation process in astrophysical environments. II - Nucleation and grain growth accompanied by chemical reaction. *Prog. Theor. Phys.* 77:1402-1410.
- Kraus M., Hulman, M., Kuzmany, H., Dennis T. J. S., Inakuma M., and Shinohara H. 1999. Diatomic metal encapsulates in fullerene cages: A Raman and infrared

- analysis of C_{84} and $Sc_2@C_{84}$ with D_{2d} symmetry. *J. Chem. Phys.* 111:7976-7984.
- Latter W. B. 1991. Large molecule production by mass-losing carbon stars: The primary source of interstellar polycyclic aromatic hydrocarbons. *ApJ* 377:187-191.
- Lodders K., and Fegley B. 1995. The origin of circumstellar silicon carbide grains found in meteorites. *Meteoritics* 30:661-678.
- Michael B. P., Nuth III J. A., and Lilleleht L. U. 2003. Zinc crystal growth in microgravity. *ApJ* 590:579-585.
- Nikolaev P., Bronikowski M. J., Bradley R. K., Rohmund F., Colbert D. T., Smith K. A., and Smalley R. E. 1999. Gas-phase catalytic growth of single-walled carbon nanotubes from carbon monoxide. *Chem. Phys. Lett.* 313:91-97.
- Nuth, J. A., Brearley, A. J. and Scott, E. R. D. 2005. Microcrystals and amorphous material in comets and primitive meteorites: Keys to understanding processes in the early solar system. In *Chondrites and the Protoplanetary Disk*, edited by A. N. Krot, E. R. D. Scott, and B. Reipurth, Astronomical Society of the Pacific Conference Series vol. 341, 675-699.
- Sharp C., and Wasserburg G. 1995. Molecular equilibria and condensation temperatures in carbon-rich gases. *Geochimica et Cosmochimica Acta* 59:1633-1652.
- Suchanek W. L., Libera J. A., Gogotsi Y., and Yoshimura M. 2001. Behavior of C_{60} under hydrothermal conditions: Transformation to amorphous carbon and formation of carbon nanotubes. *J. Solid State Chemistry*, 160:184-188.
- Trimm D. L. 1977. The formation and removal of coke from nickel catalyst. *Catalysis Reviews: Science and Engineering* 16:155-189.
- Yamamoto T., and Hasegawa H. 1977. Grain formation through nucleation process in astrophysical environment. *Prog. Theor. Phys.* 58:816-823.

Zhang B. L., Wang C. Z., Chan C. T., and Ho K. M. 1993. Thermal disintegration of carbon fullerenes. *Phys. Rev. B* 48:11381-11384.

Figure captions

Figure 1. Typical TEM images of carbon particles produced in (a) He 200 Torr, (b) He 150 and CO 50 Torr, and (c) CO 200 Torr.





Figure 2. HRTEM image and the corresponding ED pattern of carbon particles produced in He 150 and CO 50 Torr. Two halo rings attributed to the (100) and (110) crystallographic planes, which show that the cages are single shell structure, are visible in the ED pattern.

Figure 3. Mid-infrared spectra and typical HRTEM image of laboratory particles. (a): corresponding to the particles shown in Fig. 1(c), (b)-(d): corresponding to particles produced by Ti catalytic evaporation. The amount of Ti is larger in order (b), (c) and (d). The infrared spectra show the characteristic $19\text{ }\mu\text{m}$ (526 cm^{-1}) feature attributed to C_{60} . (e): Reference spectrum of C_{60} , which was taken from Kraus (1999). (f): typical HRTEM image of carbon particles corresponded with spectrum (d).

Figure 4. HRTEM images of carbon particles produced in (a) He 200 Torr, (b) He 150 and CO 50 Torr, and (c) CO 200 Torr.

Figure 5. Typical TEM images of TiC particles produced in (a) He 200 Torr and (b) CO 200 Torr. The thickness of a carbon mantle layer on TiC grains is greatly different.

Table 1. Feature of produced carbon grains

		1	2	3	4	5
Gas	He (Torr)	200	150	100	50	0
	CO (Torr)	0	50	100	150	200
Grain Size (nm)		50-100	50-100	50-100	50-100	50-100
Shape		Dendritic				Cluster
Surface		Smooth	Rough			Smooth
Surface cages		No				Whole
Amorphous core		Whole				No

Arrows show gradual change of left state to right state as CO partial pressure.

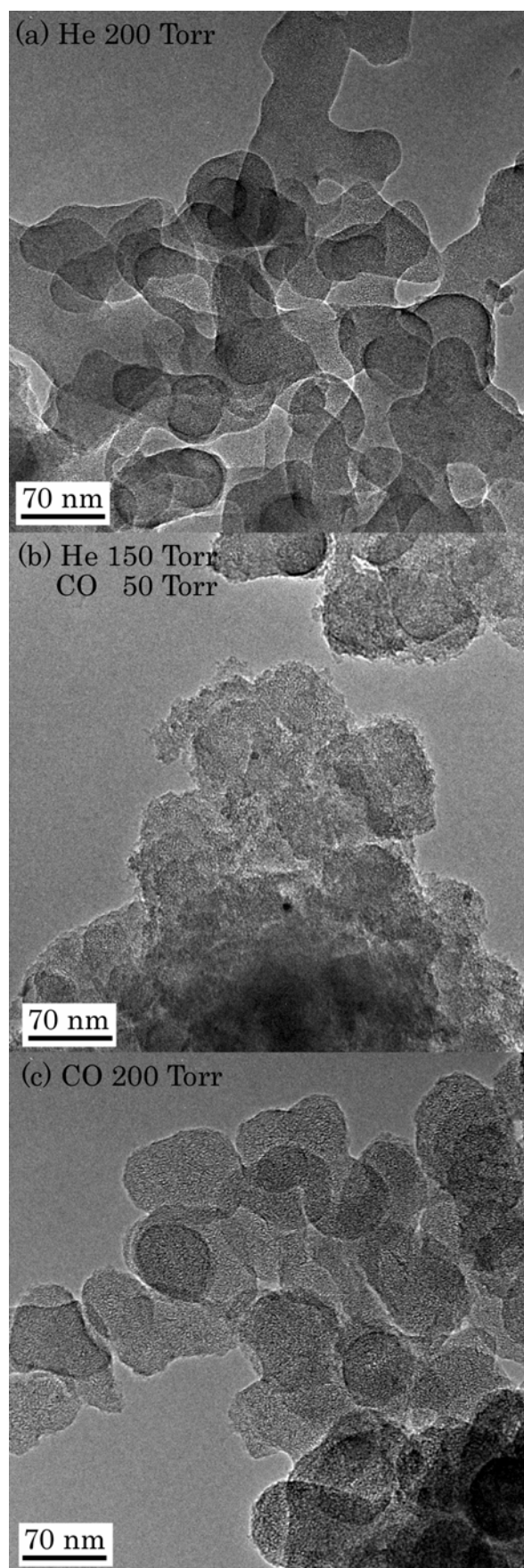


Figure 1

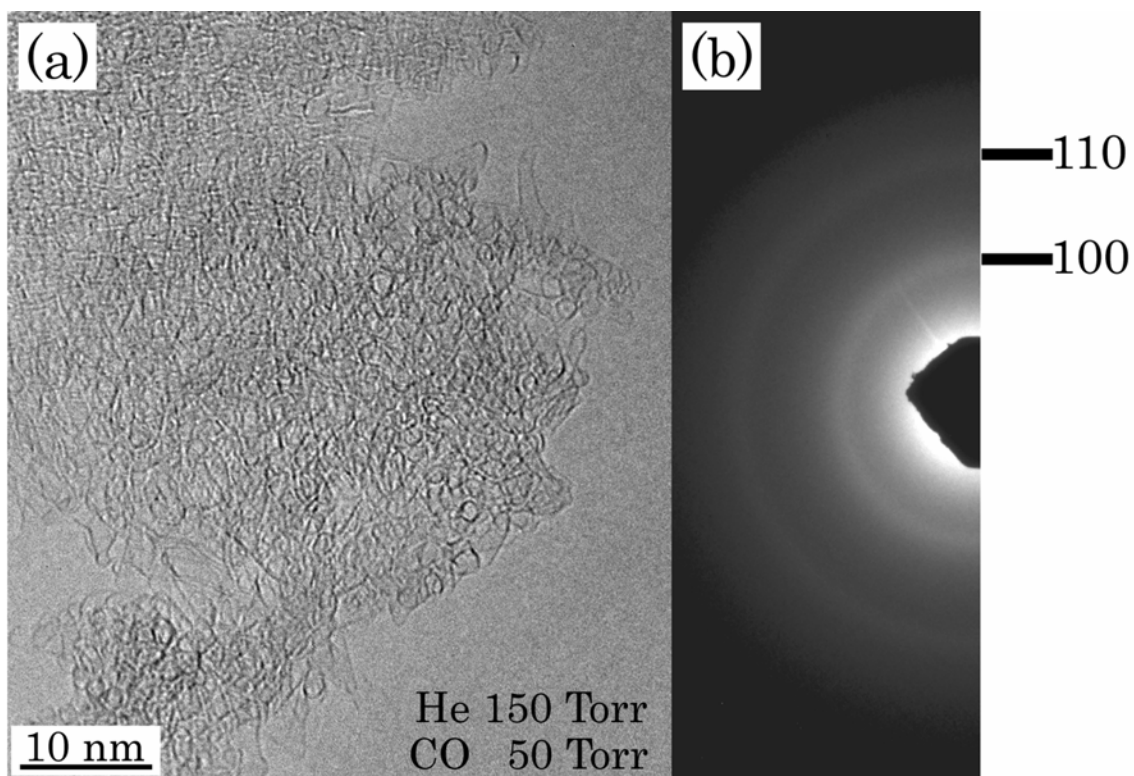


Figure 2

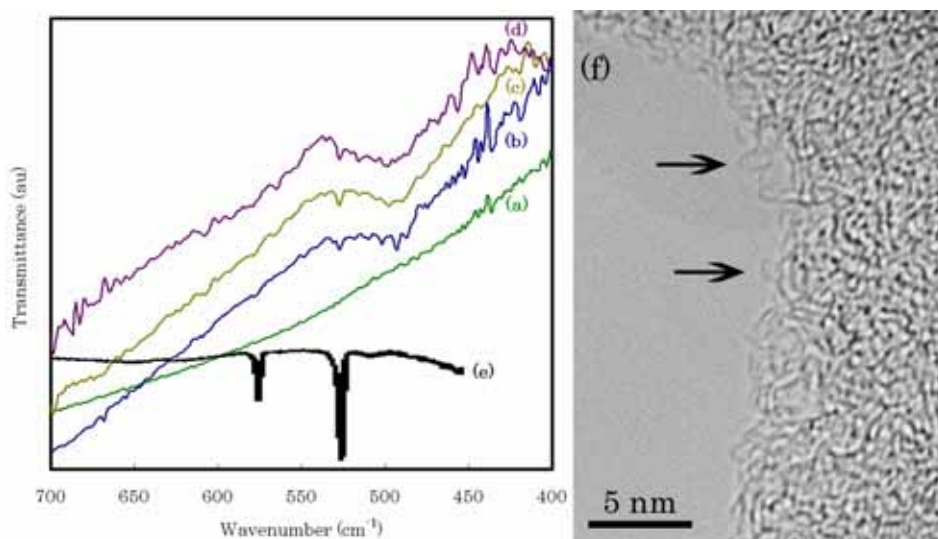


Figure 3

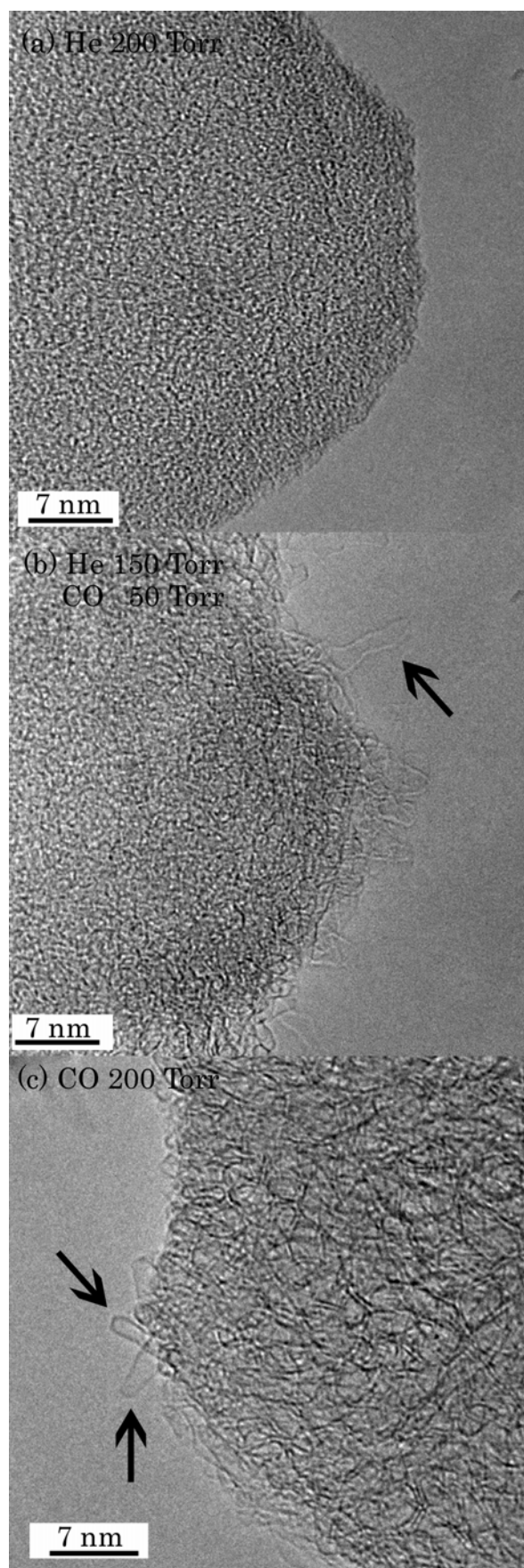


Figure 4

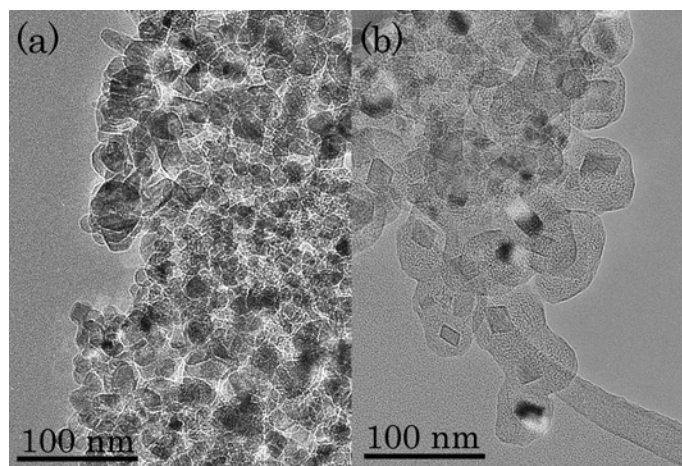


Figure 5